10 Populations of Spiking Neurons

Wulfram Gerstner

10.1 Introduction

In standard neural network theory, neurons are described in terms of mean firing rates. The analog input variable I is mapped via a nonlinear gain function g to an analog output variable $\nu = g(I)$ which may be interpreted as the mean firing rate. If the input consists of output rates ν_j of other neurons weighted by a factor w_{ij}, we arrive at the standard formula

$$\nu_i = g(\sum_j w_{ij}\, \nu_j) \tag{10.1}$$

which is the starting point of most neural network theories.

As we have seen in Chapter 1, the firing rate defined by a temporal average over many spikes of a single neuron is a concept which works well if the input is constant or changes on a time scale which is slow with respect to the size of the temporal averaging window. Sensory input in a real-world scenario, however, is never constant. Moreover reaction times are often short which indicates that neurons do not have the time for temporal averaging.

There is, however, another interpretation of 'rate' which may be used even for fast changing input. Instead of an average over time, rate may be defined as an average over a population of neurons with identical (or at least similar) properties. To distinguish this concept clearly from the temporally averaged mean firing rate, we refer to the population averaged rate as the population activity $A(t)$; cf. Chapter 1.

In this chapter we will focus on the properties of such a population of neurons. All neurons are identical, receive the same input $I(t)$ and are mutually coupled by synapses of uniform strength; cf. Figure 10.1.

Can we write down a dynamic equation in continuous time that describes the evolution of the population activity? This problem comes up in various models and has been studied by several researchers [Wilson and Cowan, 1972, 1973; Amari, 1974; Gerstner and van Hemmen, 1992, 1993, 1994; Bauer and Pawelzik, 1993; Gerstner, 1995; Pinto et al., 1996; Senn et al., 1996; Eggert and van Hemmen, 1997]. A frequently adopted solution is to replace (10.1) by a differential equation

$$\tau \frac{dA_i(t)}{dt} = -A_i(t) + g\left(\sum_j \int_0^\infty \epsilon_{ij}(s)\, A_j(t-s)\, ds\right) \tag{10.2}$$

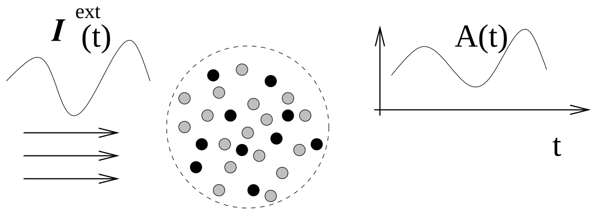

Figure 10.1. Population of neurons (schematic). All neurons receive the same input $I^{\text{ext}}(t)$ (left) which results in a time dependent population activity $A(t)$ (right).

where we have supposed that there are different populations A_i which are coupled to each other with a delay-kernel ϵ_{ij}; e.g., [Wilson and Cowan, 1972, Cohen and Grossberg, 1983, Hopfield, 1984, Pinto et al., 1996]. For stationary problems, the left-hand side of (10.2) vanishes and, with the replacement $A_i \longrightarrow \nu_i$; $\int \epsilon_{ij}(s)ds \longrightarrow w_{ij}$ we are back to (10.1).

The problem with (10.2) is that it introduces a time constant τ which is basically *ad hoc*. If we perform simulations of (10.2), what value should we take for τ?. It has been argued that τ is the membrane time constant of the neurons, an assertion which is correct in the limit of slowly changing activities only. The activity is, however, not always slowly changing. It has been shown previously that the population activity can react quasi instantaneously to abrupt changes in the input [Tsodyks and Sejnowski, 1995, van Vreeswijk and Sompolinsky, 1996]. Transients in networks of non-leaky integrate-and-fire neurons can be very short [Hopfield and Herz, 1995]. Moreover, homogeneous networks may be in an oscillatory state where all neurons fire exactly at the same time; e.g., [Mirollo and Stogatz, 1990; Gerstner and van Hemmen, 1993; Gerstner et al., 1996; Somers and Kopell, 1993; van Vreeswijk et al., 1994; Hansel, 1995; Terman and Wang, 1995]. In this case, the population activity changes rapidly between zero and a very high activity. These phenomena are inconsistent with a differential equation of the form (10.2).

In this chapter, we will analyze the population dynamics and derive a dynamic equation which is exact in the limit of a large number of neurons. The relevant equation is an integral equation with interesting properties. We focus on three special cases and discuss them in turn.

(i) How does a population of neurons react to a fast change in the input? We show that, during the initial phase of the transient, the population activity reacts instantaneously [Tsodyks and Sejnowski, 1995]. The end of the transient is, on the other hand, rather slow and indeed characterized by the membrane constant τ.

(ii) What are the conditions for exact synchrony in the firing of all neurons? We show that neurons are 'locked' together, if firing occurs while the postsynaptic potential is rising [Gerstner et al., 1996].

(iii) What are the conditions to make the neurons fire in an optimally asynchronous manner? We discuss why, without noise, asynchronous firing is almost always unstable [Abbott and van Vreeswijk, 1993; Gerstner and van Hemmen, 1993; Gerstner, 1995]. We show that with a proper choice of the delays and a sufficient amount of noise the state of asynchronous firing can be stabilized [Gerstner and van Hemmen, 1994; Gerstner, 1998].

The integral equation of the dynamics allows us to discuss all of the above three phenomena from a unified point of view.

Studies of population activity have a fairly long history. Wilson and Cowan [Wilson and Cowan, 1972] described the population activity by an integral equation which they subsequently approximated by a differential equation similar to (10.2). Other researchers have developed population equations which are formulated as maps for homogeneous [Gerstner and van Hemmen, 1992; Bauer and Pawelzik, 1993] or inhomogeneous populations [Senn et al., 1996]. In this chapter we review the population equations in *continuous* time developed in detail in [Gerstner and van Hemmen, 1992, 1994; Gerstner, 1995]. Some of the arguments follow closely the text of [Gerstner, 1998].

10.2 Model

Our discussion starts from the spike response model, our generic neuron model introduced in Chapter 1. We consider the variant of a neuron with short-term memory, Section 1.2.1., Equation (1.16), and allow for noise in the reset; cf. Section 1.2.3.3. Equation (1.55). For the sake of convenience, we recall the neuronal equation. A neuron i fires if its membrane potential ("state variable") u_i hits the threshold ϑ. The membrane potential is of the form

$$u_i(t) = \eta(t - \hat{t}_i) + h(t) \tag{10.3}$$

where $\hat{t}_i$ is the most recent firing time of neuron i, the kernel $\eta(s)$ is a (negative) contribution due to refractoriness and

$$h(t) = \sum_{j\in\Gamma_i} \sum_{t_j^{(f)}\in\mathcal{F}_j} w_{ij}\epsilon(t - t_j^{(f)}) + J^{\text{ext}} \int_0^\infty \tilde{\epsilon}(s) I^{\text{ext}}(t-s)ds \tag{10.4}$$

is the postsynaptic potential caused by firings $t_j^{(f)}$ of presynaptic neurons $j \in \Gamma_i$ or by external input $I^{\text{ext}}(t)$.

Since we are interested in a homogeneous population of neurons, the kernels η, ϵ, and $\tilde{\epsilon}$ have no indices i, j and all neurons receive the same input $I^{\text{ext}}(t)$. Moreover, the interaction strength between the neurons is uniform

$$w_{ij} = \frac{J_0}{N} \tag{10.5}$$

where J_0 is a parameter. The interaction strength scales with one over the number N of neurons so that the total input remains finite in the limit of $N \to \infty$.

The theory we are going to discuss is valid for arbitrary response kernels ϵ. For simulations of the model, we usually take a simple response kernel with a small number of parameters

$$\epsilon(s) = \begin{cases} 0 & \text{for} \quad s < \Delta^{\text{ax}} \\ \frac{s-\Delta^{\text{ax}}}{\tau^2} \exp\left(-\frac{s-\Delta^{\text{ax}}}{\tau}\right) & \text{for} \quad s \geq \Delta^{\text{ax}} \end{cases} \tag{10.6}$$

Here $\Delta^{\rm ax}$ is the axonal delay and τ is a membrane time constant. The normalization is $\int \epsilon(s) ds = 1$ as desired. For the external input we take in the simulations

$$\tilde{\epsilon}(s) = \frac{1}{\tau}\, \exp\left(-\frac{s}{\tau}\right)\, \mathcal{H}(s) \tag{10.7}$$

with the same time constant τ as in (10.6). As always, $\mathcal{H}(s)$ is the Heaviside step function with $\mathcal{H}(s) = 0$ for $s \le 0$ and $\mathcal{H}(s) = 1$ for $s > 0$.

We mentioned already that we allow for noise in the reset. Specifically, we consider a refractory kernel

$$\eta(s) = \begin{cases} 0 & \text{for} \quad s \le 0 \\ -\eta_0 \exp\left(r/\tau\right)\, \exp\left(-s/\tau\right) & \text{for} \quad s > 0 \end{cases} \tag{10.8}$$

where r is a random variable with zero mean. After each spike, a new value of r is drawn randomly from a Gaussian distribution $\mathcal{G}_\sigma(r)$ with variance $\sigma \ll \tau$. In the language of the integrate-and-fire neuron, we can describe the effect of r as a stochastic component in the value of the reset potential; cf. Chapter 1, Section 1.2.3. In the language of the Spike Response Model, we may say that a value of $r \neq 0$ shifts the response kernel horizontally along the time axis.

This is seen most easily in the following scenario. Let us consider a single neuron with constant external input I_0 and $\vartheta > 0$. There is no input from other neurons ($J_0 = 0$). After some transient the postsynaptic potential is $h_0 = J^{\rm ext} I_0$ where, as always, we have assumed a normalization $\int \tilde{\epsilon}(s) ds = 1$. Given a constant input potential $h_0 > \vartheta$, the neuron fires regularly with some period T_0. For neurons with short memory, we calculate the period from (10.3) and the threshold condition $u(t) = \vartheta$. This yields

$$\eta(T_0) = \vartheta - h_0 \tag{10.9}$$

and with (10.8)

$$T_0 = \tau\, \ln \frac{\eta_0}{h_0 - \vartheta} \qquad \text{for } h_0 > \vartheta\,. \tag{10.10}$$

What happens in the presence of noise? The period T_r for a given value of r is again found from the threshold condition $\eta(T_r) = \vartheta - h_0$. We use (10.8) and find

$$T_r = T_0 + r\,. \tag{10.11}$$

Thus the Gaussian distribution $\mathcal{G}_\sigma(r)$ of the noise variable r maps directly to a Gaussian distribution of the intervals around the mean T_0.

In order to formalize this idea, we use the notation introduced in Chapter 1, Section 1.2.3. We want to calculate the probability density $P_{h_0}(t|\hat{t})$ that the next spike occurs at time t given that the last spike was at $\hat{t}$ and the external input potential is h_0. From (10.11) we get the answer

$$P_{h_0}(t\,|\,\hat{t}) = \mathcal{G}_\sigma(t - \hat{t} - T_0) \tag{10.12}$$

where T_0 is the interval in the noiseless case. In particular, for noiseless neurons ($\sigma \to 0$), the right-hand side of (10.12) reduces to a Dirac δ-function,

$$\lim_{\sigma\to 0} P_{h_0}(t\,|\,\hat{t}) = \delta(t - \hat{t} - T_0) \tag{10.13}$$

as it should be. We will make repeated use of (10.12) and (10.13) throughout this chapter.

As noted in chapter 1, the Spike Response Model with the specific kernels (10.8) and (10.6), is closely related to the integrate-and-fire model. Specifically, the response kernel (10.6) corresponds to a synaptic time constant $\tau_s = \tau_m = \tau$ (where τ_m is the membrane time constant) and an additional axonal transmission delay Δ^{ax}. To make the models fully equivalent, we should consider a sum over the η's in order to include effects of earlier spikes, but here we restrict ourselves to the short-term memory approximation. For the numerical analysis later on, we have adjusted the threshold ϑ so that the interval T_0 is exactly $T_0 = 2\tau$. In this case, $e^{-T/\tau} \ll 1$ and therefore $\eta(nT_0) \ll \eta(T_0)$, so that the effect of the earlier spikes can indeed be neglected.

10.3 Population Activity Equation

We consider a homogeneous and fully connected network of spiking neurons in the limit of $N \to \infty$. We aim for a dynamic equation which describes the evolution of the population activity over time. Let us recall the definition of the population activity from chapter 1, Section 1.1.2.3. In any short interval Δt, we count the total number of spikes n_{act} emitted by all neurons in the population

$$n_{\mathrm{act}}(t) = \sum_{i=1}^{N} \sum_{t_i^{(f)} \in \mathcal{F}_i} \int_{t-\Delta t}^{t} \delta(t' - t_i^{(f)})\, dt' \,. \tag{10.14}$$

The population activity may formally be defined as

$$A(t) = \lim_{N\to\infty} \lim_{\Delta t \to 0} \frac{1}{\Delta t} \left[\frac{n_{\mathrm{act}}(t)}{N} \right] \,. \tag{10.15}$$

A different way of writing this is

$$A(t)\, dt = \lim_{N\to\infty} \frac{1}{N} \sum_{i=1}^{N} \delta(t - t_i^{(f)})\, dt \quad . \tag{10.16}$$

10.3.1 Integral Equation for the Dynamics

The dynamics of the population activity is given by the integral equation

$$A(t) = \int_{-\infty}^{t} P_h(t\,|\hat{t})\, A(\hat{t})\, d\hat{t} \,. \tag{10.17}$$

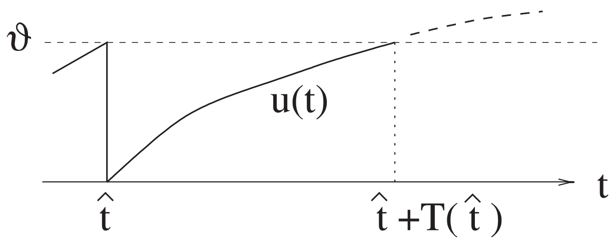

Figure 10.2. Threshold condition and definition of the inter-spike interval.

A detailed derivation is given in [Gerstner and van Hemmen, 1992, 1994; Gerstner, 1993, 1995]. Intuitively, (10.17) is easy to understand. The kernel $P_h(t\,|\,\hat{t})$ is the probability density that the next spike of a neuron which is under the influence of a potential $h(t)$ occurs at time t given that its last spike was at $\hat{t}$. The number of neurons which have fired at $\hat{t}$ is proportional to $A(\hat{t})$ and the integral runs over all times in the past.

To get a better understanding of (10.17), let us consider the noise-free case. The probability density reduces to a Dirac δ-function,

$$P_h(t\,|\,\hat{t}) = \delta[t - \hat{t} - T(\hat{t})] \tag{10.18}$$

where $T(\hat{t})$ is the interspike interval given by the threshold condition

$$T(\hat{t}) = \min\{(t - \hat{t})\,|\,u(t) = \vartheta;\, t > \hat{t}\}\,. \tag{10.19}$$

In words, the interval T is given by the first threshold crossing after the spike at $\hat{t}$; cf. Figure 10.2.

We recall that $u(t) = \eta(t - \hat{t}) + h(t)$ is the membrane potential defined in (10.3) with h defined in (10.4). Making use of Dirac's δ-function notation, we can rewrite (10.4) in the form

$$h(t) = J_0 \int_0^\infty \epsilon(s) \left[\frac{1}{N}\sum_{j=1}^{N} \sum_{t_j^{(f)} \in \mathcal{F}_j} \delta(t - t_j^{(f)} - s)\right] ds + \tag{10.20}$$
$$J^{\text{ext}} \int_0^\infty \tilde{\epsilon}(s) I^{\text{ext}}(t-s)\, ds$$

where we have used $w_{ij} = J_0/N$. In the limit of $N \to \infty$, the term in the square brackets reduces to the population activity A defined in (10.16). Thus, in the limit $N \to \infty$, (10.20) becomes

$$h(t) = J_0 \int_0^\infty \epsilon(s)\, A(t-s)\, ds + J^{\text{ext}} \int_0^\infty \tilde{\epsilon}(s)\, I^{\text{ext}}(t - s\,) ds\,. \tag{10.21}$$

The equation (10.17) with the kernel $P_h(t\,|\,\hat{t})$ calculated for the potential h given by (10.21) defines the dynamics in a homogeneous network of spiking neurons with short-term memory. We remark that even though (10.17) looks linear, it is in fact a highly non-linear equation because the kernel $P_h(t\,|\,\hat{t})$ depends on h and h in turn depends again on the activity via (10.21).

A generalization of (10.17) and (10.21) to several populations is possible. As a short detour, let us consider a network which is subdivided into several pools. Within each pool, neurons are homogeneous. The activity of a pool m is $A_m(t)$. Neurons within each pool are connected with strength $w_{mm} = J_{mm}/N_m$ where N_m is the number of neurons in pool m. A neuron in pool m receives input from all neuron in pool n with strength $w_{mn} = J_{mn}/N_n$. The total input potential to pool m is then given by a straightforward generalization of (10.21) [Gerstner, 1995]

$$h_m(t) = \sum_n J_{mn} \int_0^\infty \epsilon(s)\, A_n(t-s)\, ds\,. \tag{10.22}$$

For the sake of simplicity we have suppressed the term accounting for external input. The dynamic equation (10.17) remains unchanged but has to be applied to each pool separately.

In the following sections we concentrate on the dynamics of a single pool with homogeneous internal and external coupling J_0 and $J^{\rm ext}$, respectively.

10.3.2 Normalization

A final remark concerns the proper normalization of the activity. It is clear that (10.17) is invariant under a rescaling of the activity $A \longrightarrow c\,A$ with some constant c. Thus the variable A in (10.17) is not necessarily the activity defined in (10.15).

In order to find the correct normalization we use the following consideration [Gerstner, 1995]. We have defined $P_h(t\,|\,\hat{t})$ as the probability density that a neuron which has fired at $\hat{t}$ and is under the influence of an input h fires again at t. The integral $\int_{\hat{t}}^t P_h(s\,|\,\hat{t})\, ds$ gives therefore the probability that it fires its next spike sometime between $\hat{t}$ and t. Consequently, we can define a survival probability

$$S_h(t\,|\,\hat{t}) = 1 - \int_{\hat{t}}^t P_h(s\,|\,\hat{t}) ds\,, \tag{10.23}$$

i.e., the probability that a neuron which is under the influence of h and has fired its last spike at $\hat{t}$ 'survives' without firing up to time t.

Let us now return to our homogeneous network and consider the state at time t. The portion of neurons which have fired their *last* spike between t_0 and t is

$$\int_{t_0}^t S_h(t\,|\,\hat{t})\, A(\hat{t})\, d\hat{t}\,. \tag{10.24}$$

In a network which is not completely noise free, all neurons have fired at *some* point in the past, thus

$$\int_{-\infty}^t S_h(t\,|\,\hat{t})\, A(\hat{t})\, d\hat{t} = 1\,, \tag{10.25}$$

which must hold at any arbitrary time t. (10.25) is the desired normalization condition [Gerstner, 1995]. It is sufficient to impose (10.25) at one instant $\tilde{t}$. The dynamics (10.17) automatically assures that the normalization remains correct for all times $t > \tilde{t}$. In fact, taking the derivative of (10.25) yields the activity dynamics (10.17).

In the following sections the population equations (10.17) and (10.25) are analyzed for various scenarios.

10.4 Noise-Free Population Dynamics

We study (10.17) in the noiseless case. As mentioned above, the integration kernel $P_h(t \,|\, \hat{t})$ reduces for noiseless neurons to a δ-function,

$$A(t) = \int_{-\infty}^{t} \delta(t - \hat{t} - T(\hat{t}))\, A(\hat{t})\, d\hat{t}\,. \tag{10.26}$$

Here $T(\hat{t})$ is the interval given implicitly by the threshold condition (10.19). When performing the integration we have to take the dependence of T upon $\hat{t}$ into account. If we do so, we find

$$A(t) = k(t)\, A(t - T) \tag{10.27}$$

where T is the interval calculated from (10.19). The scaling factor k on the right-hand side of (10.27) is given by [Gerstner, 1998]

$$k(t) = \left[1 + \frac{dT}{d\hat{t}}\right]^{-1} = 1 + \frac{h'(t)}{\eta'(T)}. \tag{10.28}$$

As usual, the primes on h and η denote a temporal derivative.

The meaning of the factor k is illustrated in Figure 10.3. A neuron which has fired at $\hat{t}$ will fire again at $t = \hat{t} + T(\hat{t})$. Another neuron which has fired slightly later at $\hat{t} + \delta t'$ fires its next spike at $t + \delta t$. If the input potential is constant between t and $t + \delta t$, then $\delta t = \delta t'$. If, however, h increases between t and $t + \delta t$ as is the case in Figure 10.3, then the firing time difference is reduced.

The compression of firing time differences is directly related to an increase in the activity A. To see this, we note that all neurons which fire between $\hat{t}$ and $\hat{t} + \delta t'$, must fire again between t and $t + \delta t$. This is due to the fact that the network is homogeneous and the mapping $\hat{t} \to t = \hat{t} + T(\hat{t})$ is monotonous. If firing time differences are compressed, the population activity increases.

Let us now return to Equation (10.28). For a standard integrate-and-fire type neuron, the kernel η has slope $\eta'(s) > 0$ for all $s > 0$; cf. Equation (10.8). An input with $h' > 0$ implies then, because of (10.27), an increase of the activity: $k > 1 \Longrightarrow A(t) > A(t - T)$. Similarly, $h' < 0$ causes a decrease of the activity ($k < 1$). This is a rather general property of the noise-free equations which will be exploited in the following two sections.

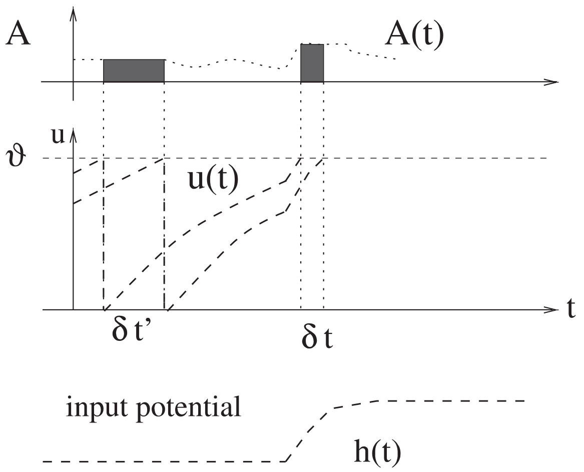

Figure 10.3. A change in the input potential h with positive slope $h' > 0$ (bottom trace) shifts neuronal firing times closer together (middle trace). As a result, the activity $A(t)$ is higher at $t = \hat{t} + T(\hat{t})$ than it was at time $\hat{t}$. Taken from [Gerstner, 1998].

10.5 Locking

As a first application of the population equations (10.17), let us reconsider, from the point of view of population dynamics, the 'locking theorem' developed in Gerstner et al. [Gerstner et al., 1996].

The question we are going to study is the following. We consider a homogeneous network with constant external input I_0. What are typical states? If we perform simulations of the neuron model, we find two extreme situations. The first one is that, after some time, the neurons all fire exactly in synchrony. This is called an oscillatory state and the phenomenon of firing together is called locking. The activity in this case exhibits a large-amplitude oscillation; cf. Figure 10.4.

The other extreme situation is that of a network where neuronal firing is maximally asynchronous so that the population activity is, apart from minor fluctuations, constant. We call this a state of asynchronous firing; see Section 10.7.

The question now is the following. If we know the parameters of the neurons and the neuronal couplings, can we predict whether the system will end up in a synchronous 'locked' state or whether it will end up in an asynchronous state? More precisely, what are the conditions on the parameters for existence and stability for a locked state? This is the question which we will address in this section. The analysis of the asynchronous state which is slightly more complicated is delayed to Section 10.7.

Before we start we note that the situation with constant external input is equivalent to a network without input but slightly different threshold. After some initial transient the external input gives a constant contribution $h^{\text{ext}} = J^{\text{ext}} I_0$ to the membrane potential. We can include this part in the threshold by the replacement $\vartheta - h^{\text{ext}} \longrightarrow \vartheta$ and treat the network as having no external input.

a)

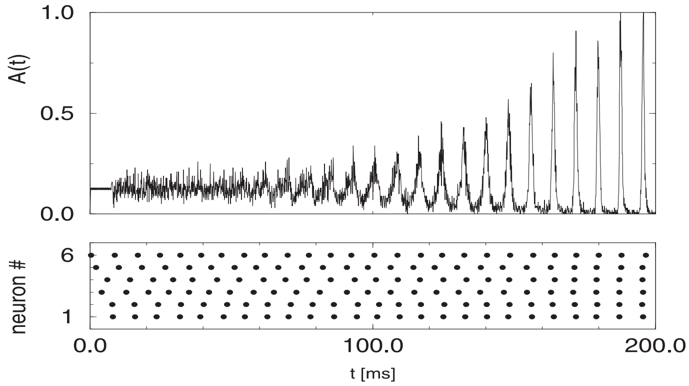

b)

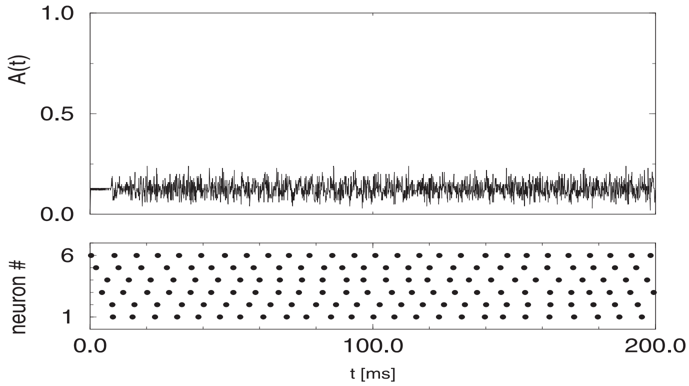

Figure 10.4. Two typical networks states: Oscillations (a) or asynchronous firing (b). In both cases the upper graph shows the networks activity $A(t)$ and the lower graph the spike trains of 6 neurons in the network. Each spike is denoted by a black dot. The initialization of the network occurs during the first 8 ms; afterwards the system runs freely without external input. Simulation parameters: network of 1000 neurons with $\tau = 4$ ms, $\vartheta = -0.01$, $J_0 = 1$ ms, $\sigma = 0.5$ ms. Delay $\Delta^{\mathrm{ax}} = 7$ ms in (a) and 3 ms in (b).

10.5.1 Locking Condition

Our considerations will focus on locking in populations of noiseless neurons. In order to analyze the stability of oscillatory states as in Figure 10.4a, we start from the noise-free dynamic equations (10.27). We assume that the network is already very close to perfect synchronization and fires nearly regularly with period T. In order to keep the arguments transparent, let us assume that the population activity for times $t < T/2$ can be approximated by a sequence of square pulses

$$A(t) = \sum_{n=-m}^{0} \frac{1}{2\delta^n} \mathcal{H}(t - nT + \delta^n)\, \mathcal{H}(nT + \delta^n - t)\,, \tag{10.29}$$

where m is some small integer, say $m = 3$, and $\mathcal{H}(.)$ denotes the Heaviside step function with $\mathcal{H}(s) = 1$ for $s > 0$ and $\mathcal{H}(s) = 0$ for $s \leq 0$. The

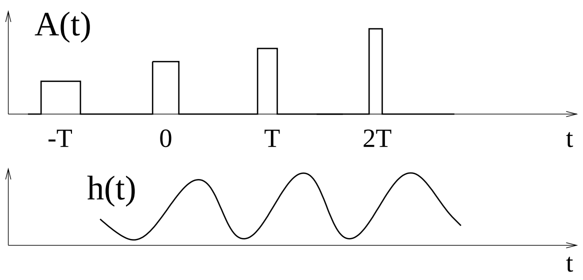

Figure 10.5. A sequence of square activity pulses contracts to δ-pulses, if firing occurs always when the input potential h is rising (schematic).

parameters δ^n with index n are assumed to be small, i.e., $\delta^n \ll T$ where T is the period.

Equation (10.29) is an 'Ansatz' which is ad hoc. We now have to check whether (10.29) is consistent with the noise-free population dynamics (10.27). More precisely, we ask the following question; cf. Figure 10.5. Is there some period T and some sequence δ^n for $n = -m, -m+1, \dots, 0, 1, 2, \dots$ so that the sequence of square pulses described by (10.29) continues for $t > T/2$? We are going to determine T and the sequence δ^n self-consistently. If we find $\delta^n \to 0$ for $n \to \infty$, then the square pulses contract to δ-functions and we say that a synchronous T-periodic oscillation is a stable solution.

To proceed we have to determine the potential $h(t)$. From the derivative of h we can calculate the factor k given by (10.28). The period T is found from the threshold condition $\vartheta = \eta(T) + h(t)$. Let us see how this works.

To get h, we put (10.29) in (10.21). Under the condition that $\delta^n \ll T$, we can easily perform the integration. To first order in δ^n we find

$$h(t) = \sum_{n=0}^{n_{\max}} J_0\, \epsilon(t + n\,T) \;+\; \mathcal{O}\left[(\delta^n)^2\right] \tag{10.30}$$

The sum runs over all pulses back in the past. Since $\epsilon(s)$ decays off quickly for $s \gg T$, it is usually sufficient to keep only a finite number of terms, e.g., $n_{\max} = 1$ or 2.

As the next step we determine the period T. To do so, we consider a neuron in the *center* of the square pulse which has fired its last spike at $\hat{t} = 0$. Since we consider noiseless neurons the relative order of firing the neurons can not change. To make the Ansatz (10.29) consistent, the next spike of this neuron must therefore occur at $t = T$, viz. in the center of the next square pulse. We use $\hat{t} = 0$ in the threshold condition (10.19) which yields

$$T = \min\left\{ t \,|\, \eta(t) + J_0 \sum_{n=0}^{n_{\max}} \epsilon(t + n\,T) = \vartheta \right\} . \tag{10.31}$$

If a synchronized solution exists, (10.31) defines the period.

We now return to Equations (10.27) and (10.28). On the right-hand side of

(10.28), we need the derivative

$$h'(t) = J_0 \sum_{n=0}^{n_{\max}} \epsilon'(t + n\,T)\,. \tag{10.32}$$

We are interested to find out whether the amplitude of the square pulse increases or decreases over time. According to (10.27), the new value of the activity at time $t = T$ is the old value multiplied by k. Thus for $k > 1$ we have an increase, for $k < 1$ a decrease. With the kernel η given by (10.8), we have $\eta'(T) > 0$ whatever T. We therefore see immediately from (10.29) that for $h'(T) > 0$, we have $k > 1$ and the amplitude of the square pulse increases. From (10.32) and (10.27) we have the result

$$h'(T) = J_0 \sum_{n=1}^{n_{\max}+1} \epsilon'(n\,T) > 0 \quad \Longrightarrow \quad A(T) > A(0) \tag{10.33}$$

which is the essence of the locking theorem [Gerstner et al., 1996].

An increase in the amplitude should correspond to a compression of the width of the pulse. To check that this is indeed the case, let us consider one of the 'corner neurons' which has fired at $t = \pm\delta^0$. Its input potential is given by (10.30). The next spike occurs at $t = T \pm \delta^1$ where T is the period and δ^1 is determined now. We recall the threshold condition for the neuron in the center of the pulse

$$\eta(T) + h(T) = \vartheta\,. \tag{10.34}$$

For the corner neuron we have

$$\eta\left(T \pm (\delta^1 - \delta^0)\right) + h(T \pm \delta^1) = \vartheta\,. \tag{10.35}$$

An expansion to first oder in δ^1 yields

$$\delta^1 = \left[1 + \frac{h'(T)}{\eta'(T)}\right]^{-1} \delta^0\,. \tag{10.36}$$

Thus, for $h'(T) > 0$ the width of the square pulse contracts as expected. Moreover the pulse remains normalized since

$$\begin{aligned} \delta^1 &= \frac{1}{k(T)}\,\delta^0 \\ A(T) &= k(T)\,A(0) \end{aligned} \tag{10.37}$$

with $k(T) = 1 + h'(T)/\eta'(T)$. By iteration of the argument for $t = n\,T$ with $n = 2, 3, 4, \ldots$ we see that the sequence δ^n converges to zero and the square pulses approach a Dirac δ-pulse under the condition that $h'(T) = \sum_n \epsilon'(n\,T) > 0$. In words, the T-periodic synchronized solution with T given by (10.31) is stable, if the postsynaptic potential at the moment of firing is rising [Gerstner et al., 1996]. Equation (10.36) is exactly the locking equation for neurons with short memory. Generalizations to neurons with long memory (where we have to sum over several η-kernels) are straightforward but involve some more indices [Gerstner et al., 1996]. With an additional amount of effort an extension from homogeneous to weakly inhomogeneous networks is also possible [Gerstner et al., 1993, Chow, 1998]. In the following subsection we give a graphical interpretation of the locking theorem.

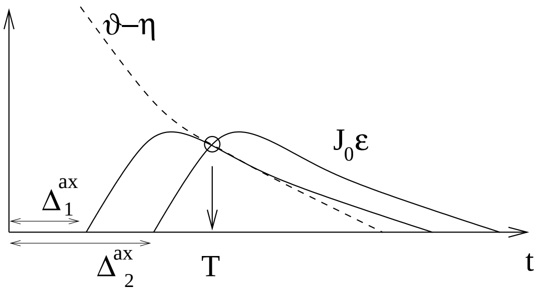

Figure 10.6. The period T of a synchronous oscillation is found from the first intersection between the total postsynaptic potential $J_0\,\epsilon(t)$ and the dynamic threshold $\vartheta - \eta(t)$. All neurons have fired synchronously at $t = 0$ and fire again $t = T$. Two different cases are shown: case 1 with short axonal delays $\Delta_1^{\rm ax}$ and case 2 with a longer transmission delay $\Delta_2^{\rm ax}$. The synchronous solution is stable if the intersection occurs where ϵ' is positive as in case 2 and is unstable in case 1. Adapted from [Gerstner et al., 1996].

10.5.2 Graphical Interpretation

In order to get a better intuitive understanding of the locking principle, let us consider a simplified scenario. We assume that all neurons have fired synchronously at $t = 0$. Let us suppose that the postsynaptic potential is rather short so that only one term in the sum on the right-hand side of (10.30) contributes, viz.,

$$h(t) = J_0\,\epsilon(t) \tag{10.38}$$

In this case the threshold condition (10.31) may be written as

$$T = \min\left\{t \mid J_0\,\epsilon(t) = \vartheta - \eta(t)\right\} . \tag{10.39}$$

Equation (10.39) has a simple interpretation. The next spike occurs when the total postsynaptic potential caused by the spikes emitted at $t = 0$ surpasses the dynamic threshold $\vartheta - \eta$. Since all neurons have identical parameters and have fired synchronously at $t = 0$, the threshold condition (10.39) is the same for all neurons and they will therefore continue to fire synchronously. Therefore, we may say that a synchronous network state exists whenever (10.39) has a solution. The locking theorem furthermore tells us that this solution is stable if the firing occurs on the rising slope of the postsynaptic potential. In Figure 10.6 we see that, in case of excitatory interaction, this is possible when the axonal transmission delay is rather long. For shorter delay values, the intersection point is on the downward slope of $J_0\epsilon$ and the synchronous solution is therefore unstable.

Since the derivation of the locking condition was rather general, we can apply our results not only to excitatory but also to inhibitory interaction. Obviously, to make the inhibitory neurons fire we need some external input I_0 which we take to be constant. It gives a contribution $h^{\rm ext} = J^{\rm ext}\,I_0$ to the membrane potential which we can either subtract from the threshold or else add to the postsynaptic potential. In Figure 10.7 we have chosen the latter possibility. We see that for inhibition with short or medium

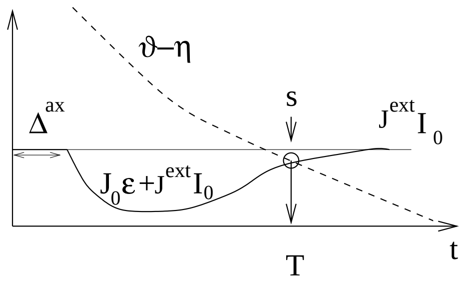

Figure 10.7. The locking argument applied to neurons with inhibitory interaction. The synchronized solution is stable since the intersection $J_0\,\epsilon(t) + J^{\rm ext} I_0 = \vartheta - \eta(t)$ occurs at a moment t when $\epsilon'(t) > 0$ (arrow marked 's'); taken from [Gerstner et al., 1996].

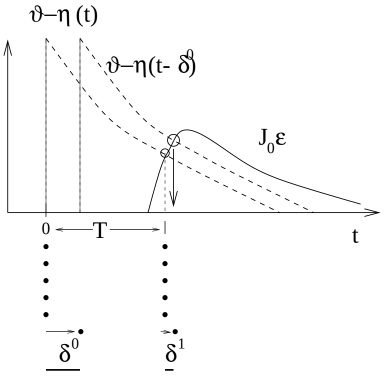

Figure 10.8. In the lower half of the figure we show schematically the spikes (marked by dots) of 6 neurons. All neurons have fired at $t = 0$ except the neuron in the bottom trace which is late by an amount δ^0. The synchonous neurons fire their next spike at time T; the late neuron becomes active at $T + \delta^1$. Note that $\delta^1 < \delta^0$ which shows that the synchronous oscillation is stable.

delays the intersection point occurs on the *rising* part of the postsynaptic potential (decreasing inhibition = increasing postsynaptic potential). The synchronous solution with period T is therefore stable.

Can we understand the condition on the slopes graphically? Let us focus on Figure 10.8. All neurons have fired synchronously at $t = 0$ except for one neuron which has fired late by an amount δ^0. The bulk of the neurons fires again at $t = T$ given by $J_0\epsilon(T) = \vartheta - \eta(T)$. The threshold of the neuron which has fired late, however, comes down with a delay δ^0 with respect to the others. Graphically this is equivalent to shifting the curve $\vartheta - \eta$ by an amount δ^0 to the right. The intersection point between $\vartheta - \eta(t - \delta^0)$ and the potential $J_0\,\epsilon(t)$ caused by the spikes of the other neurons gives the next firing time of the 'late' neuron. We see directly from Figure 10.8 that the shift δ^1 is reduced with respect to δ^0. Thus the neuron is pulled back into the collective oscillation. For $\epsilon' = 0$ we would have $\delta^1 \approx \delta^0$ and for $\epsilon' < 0$ the shift is even increased.

So far, we have always assumed that there was a finite transmission delay $\delta^{\rm ax}$. In the case of a fast rising postsynaptic potential with zero delay, the graphical construction is slightly more complicated. As soon as the neurons fire the spikes are felt by the other neurons. Apart from the spikes of the preceding cycle, we therefore have also to include the immediate effect of the spikes of the *same* cycle. The results are graphically shown in Figure 10.9. We consider the time course of the postsynaptic potential $h(t)$ and the dynamic threshold $\vartheta - \eta$ over several periods. Firings at $t = 0$, $t = T$, $t = 2T$ increase the dynamic threshold and at the same time the postsynaptic potential; cf. 10.9a. As in the preceding figure, we now assume that one of the neurons fires slightly out of tune with a time shift δ^0 which may be either positive or negative; cf. Figure 10.9b. If it fires early, we have to shift the curve $\vartheta - \eta$ to the left; if it fires late, we have to shift it to the right. We see from Figure 10.9b that for a neuron which has fired early, the next crossing is on the downward slope of the postsynaptic potential and the time shift is *increased*. For a neuron which fires late with respect to the others, the time shift is *decreased*. Thus, the synchronous solution is *locally unstable* for negative time shifts.

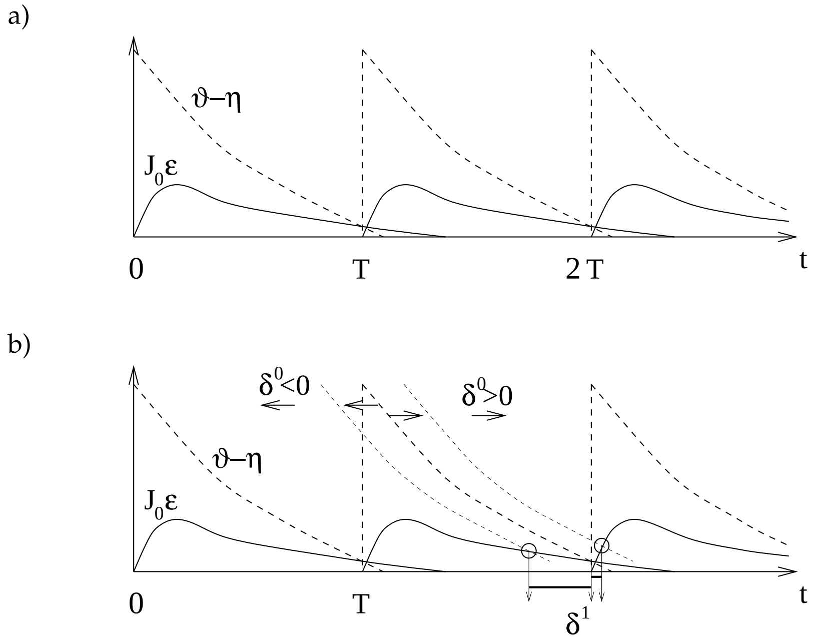

Figure 10.9. Excitatory interaction with zero delay. a) The neurons fire where the total postsynaptic potential $J_0\epsilon$ crosses the dynamic threshold $\vartheta - \eta$. The pattern repeats periodically with period T. b) For a neuron which has fired at time $t = T + \delta^0$ instead of $t = T$ the dynamic threshold is shifted by an amount δ^0 to the left (for $\delta^0 < 0$) or right (for $\delta^0 > 0$). For $\delta^0 < 0$ the time shift with respect to the synchronous firing of the other neurons increases from one cycle to the next ($|\delta^1| > |\delta^0|$). For a neuron which has fired late ($\delta^0 > 0$), the time shift is decreased ($|\delta^1| < |\delta^0|$) and it is therefore pulled back into the collective oscillation; taken from [Gerstner et al., 1996].

As shown by Mirollo and Strogatz [Mirollo and Strogatz, 1990], synchronized firing in a network with zero-delay coupling may nevertheless be *globally* stable. The reason is, that a neuron which has fired early, will fire even more early the next time and so on. After several firings, it has drifted away by nearly a full period and it now appears to be *late* with respect to the previous synchronous firing of the other neurons. As we have seen above, a neuron which fires late is then pulled back into the collective firing. The Mirollo-Strogatz model is reviewed in Chapter 11.

10.6 Transients

As a second application of the noise-free population dynamics, let us study the response of the population activity to a rapid change in the input. To keep the arguments as simple as possible, we consider an input which has a constant value I_0 for $t < t_0$ and changes then abruptly to a new value $I_0 + \Delta I$. Thus

$$I(t) = \begin{cases} I_0 & \text{for} \quad t \le t_0 \\ I_0 \ +\Delta I & \text{for} \quad t > t_0 \end{cases}$$

How does a homogeneous population of neurons react to such a step current input? In this section we try to find an answer to the above question. The arguments follow directly those developped in [Gerstner, 1998].

In order to analyze the situation, let us suppose that for $t < t_0$ the network is in a state of *incoherent* firing. In other words, all neurons fire at the same mean firing rate, but their spikes are not synchronized. Rather the firing times are maximally spread out over time. Such a state has been called the 'splay phase' [Chow, 1998]. In the limit of $N \to \infty$, the population activity is then a constant $A(t) = A_0$. In Section 7 we will study the conditions under which a state of incoherent firing can be a stable state of the system. Here we just assume the we can set the parameters so that the network fires indeed asynchronously and with constant activity.

In order to keep the arguments simple, we assume that the neurons are not coupled to each other. For $t \le t_0$ all neurons receive a constant input potential $h_0 = J^{\text{ext}}\, I_0$ since $\int \tilde{\epsilon}(s) ds = 1$. For $t > t_0$, the input potential changes due to the additional current ΔI. Thus

$$h(t) = \begin{cases} h_0 & \text{for} \quad t \le t_0 \\ h_0 \ + J^{\text{ext}} \Delta I \int_0^{t-t_0} \tilde{\epsilon}(s) ds & \text{for} \quad t > t_0 \end{cases}$$

In the noiseless case, neurons which receive a constant input potential h_0 fire regularly with a period T_0 given by

$$\eta(T_0) = \vartheta - h_0 \,. \tag{10.40}$$

The mean activity A_0 for $t < t_0$ is simply $A_0 = 1/T_0$. The reason is that, for a constant activity, averaging over time and averaging over the population must be the same. To see this consider a long measurement interval Δta. For $\Delta t \gg T_0$ the populations of $N \gg 1$ neurons will emit $n_{\text{act}} = N\, \Delta t/T_0$ spikes in the time Δt. Taking the limits $N \to \infty$ and $\Delta \to 0$ yields the activity $A_0 = 1/T_0$; cf. (10.15).

Let us now return to the population dynamics. We recall the formulas (10.27) and (10.28) for the noiseless case

$$A(t) = \left[1 + \frac{h'(t)}{\eta'(T)}\right] A(t-T) \tag{10.41}$$

where T is implicitly given by the threshold condition (10.19). For $t < t_0$, the input potential is constant $h(t) = h_0$, thus $h' = 0$ and $T = T_0$. Equation (10.41) then yields $A(t) = A(t - T_0)$ as it should be for a constant activity A_0.

What happens for $t > t_0$? In order to use (10.41), we have to calculate the derivative $h'(t)$. We find from (10.40)

$$h'(t) = J^{\text{ext}}\, \Delta I\, \tilde{\epsilon}(t - t_0)\,. \tag{10.42}$$

If the change ΔI in the input current is small, we expect that the interspike interval T changes only slightly. In order to keep the arguments transparent, we make a zero order approximation and set $A(t-T) \approx A(t-T_0)$ and $\eta'(T) \approx \eta'(T_0)$. The population equation (10.41) then yields

$$A(t) = [1 + a\,\tilde{\epsilon}(t - t_0)]\; A(t - T_0) \tag{10.43}$$

with a constant $a = J^{\text{ext}}\, \Delta I/\eta'(T_0)$.

Let us now concentrate on the initial phase of the transient $t_0 < t < t_0 + T_0$. For a t taken from that interval, we have $A(t - T_0) = A_0$ which simplifies the right-hand side of (10.43):

$$A(t) = A_0 + \Delta A\, \tilde{\epsilon}(t - t_0) \quad \text{for}\;\; t_0 < t < t_0 + T_0 \tag{10.44}$$

with $\Delta A = a\, A_0$. Thus the shape of the initial transient reflects the time course $\tilde{\epsilon}$ of the postsynaptic potential caused by external input.

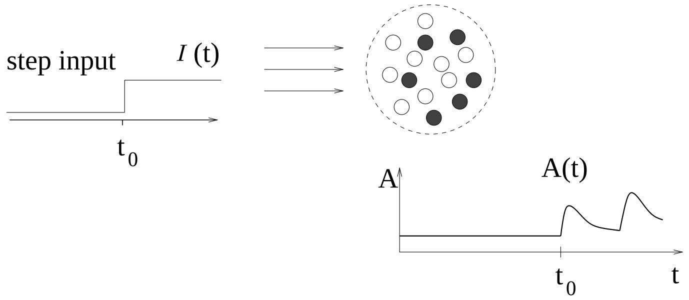

Figure 10.10. Response of a population of neurons to a step input (schematic).

To appreciate the consequences, let us consider the kernel (10.7). The response of the input *potential* to the step current (10.40) is given by (10.40) and has the typical low-pass filter characteristic $h(t) = h_0 + J^{\text{ext}} \Delta I\, [1 - \exp[-(t - t_0)/\tau]$ for $t > t_0$. The population activity, however, reacts *instantaneously* to the step current. In our little example, the initial transient is

$$A(t) = A_0 + \Delta A\, \frac{1}{\tau}\, \exp\left(-\frac{t - t_0}{\tau}\right) \mathcal{H}(t - t_0) \quad \text{for}\;\; t_0 < t < t_0 + T_0 \tag{10.45}$$

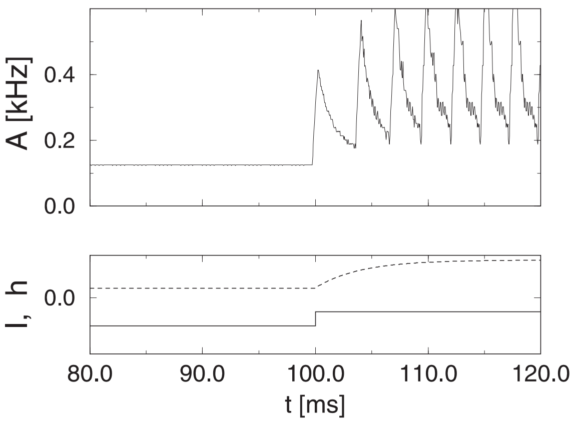

Figure 10.11. Simulation result. The population activity (top) in response to a step input current (bottom, solid line). The population activity reacts instantaneously to the step input, even though the input potential h (dashed line) caused by the step current responds only slowly. Simulation parameters: 100 neurons withoug interaction ($J_0 = 0$) in the limit of no noise $\sigma = 0$. In order to smooth out numerical artefacts the activity has been plotted after taking a running averag over 1 ms. Taken from [Gerstner, 1998].

where $\mathcal{H}(.)$ is the Heaviside step function. This implies in particular that the dynamic rate model (10.2) defined by a differential equation with time constant τ can not describe the initial phase of the transient. This is the precise meaning of the claim made in the introduction. A simulation in Figure 10.11 confirms the rapid initial response of the population.

Equation (10.45) is valid only during the initial phase of the transient. As soon as every neuron has fired once, the activity on the right-hand-side of (10.43) can no longer be considered constant. For $t > t_0 + T_0$ we must therefore include the first order correction $\Delta A\, \tilde{\epsilon}(t - t_0)$, for $t > t_0 + 2T_0$ a second order correction and so forth. The consequences are shown schematically in Figure 10.10. A simulation result is shown in Figure 10.11. The peaks in the activity repeat and slowly build up towards a periodic state. The peaks occur at times t_0, t_1, t_2 with $t_k \approx t_0 + k\,T$. We can estimate the sequence of peak values from the iteration

$$A(t_{k+1}) = A(t_k)\,\left[1 + \frac{h'(t_{k+1})}{\eta'(T_0)}\right]\,. \tag{10.46}$$

In our little example discussed above, we have $h' \propto \exp[-(t - t_0)/\tau]$, and the solution of (10.46) is therefore of the form

$$A(t_k) = A_{\rm fin}\,\left[1 - \exp\left(-\frac{t_k - t_0}{\tau}\right)\right]\,. \tag{10.47}$$

Equation (10.47) shows that the sequence of peaks follows the same exponential time course as the input potential h. Similarly, the temporally *averaged* activity would follow an exponential time course. Taking a temporal averages does, of course, lead back to rate models. Our detailed approach outlined above shows, however, that the initial transient of the activity is much faster than that predicted from an exponential activity dependence.

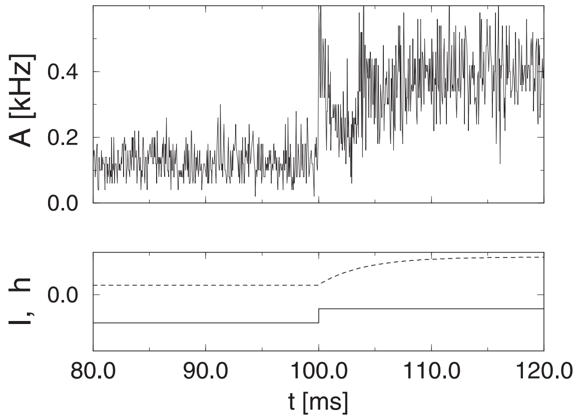

Figure 10.12. Simulation result. Same as in the previous figure but at a noise level of $\sigma = 1$. Taken from [Gerstner, 1998].

So far, we have considered noiseless neurons. In the presence of noise, subsequent pulses get smaller and broader and the network approaches a new incoherent state; cf. Fig 10.12. If, in addition, there is also some interaction $J_0 \neq 0$ between the neurons, then the value of the new stationary state is shifted. A particularly interesting state is inhibitory interaction $J = -1$. In this case the new value of the stationary activity for $t > t_0$ is only slightly higher than that for $t < t_0$. The fast transient with a sharp first peak is clearly visible and marks the moment of input switching. Fast switching has previously been seen in heterogeneous networks with balanced excitation and inhibition [Tsodyks and Sejnowski, 1997, van Vreeswijk and Sompolinsky, 1996]. Here it is demonstrated and analyzed for homogeneous networks.

Finally we may wonder whether we can understand fast switching intuitively. Before the abrupt change the input was stationary. For the theoretical analysis, we have assumed that the population was in a state of *incoherent* firing. For the simulations, parameters where chosen so that neurons fire asynchronously. Incoherent firing was defined as a state where neuronal firing times are spread out maximally. Thus some of the neurons fire, others are in the refractory period, again others approach the threshold. There is always a group of neuron whose potential is just below threshold. An increase in the input causes those neurons to fire immediately - and this accounts for the strong population response during the initial phase of the transient.

10.7 Incoherent Firing

We have seen in the preceding section that a population of neurons reacts instantaneously to a change in the input – given that the network is in a state of *incoherent* firing. What are the conditions for incoherent firing be a stable state of the network dynamics? This is the question we study in this subsection.

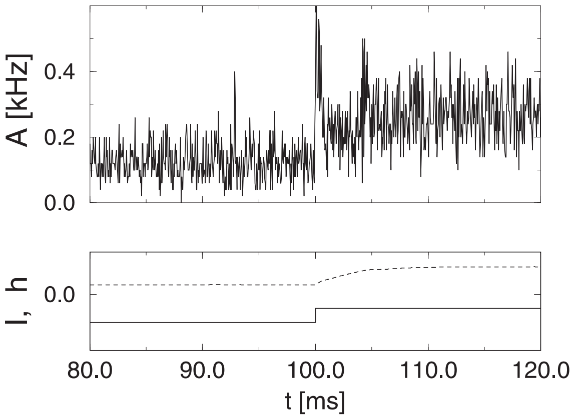

Figure 10.13. Simulation result. Same as in the previous figure but with inhibitory interaction ($J_0 = -1$); noise parameter $\sigma = 1$. Taken from [Gerstner, 1998].

We will proceed in three steps. First we want to show the *existence* of states of incoherent firing and calculate the value of the activity A_0. Second, we study the *stability* of incoherent firing. The stability analysis involves some lengthy calculations which can be found in subsection 2.7.2.1. and may be omitted by those readers who are not interested in the details. Finally, we apply the stability results to a specific model system and discuss the results. The text follows the arguments developed in [Gerstner, 1993, 1995, 1998].

10.7.1 Determination of the Activity

Incoherent firing may be defined as a macroscopic firing state with constant activity $A(t) = A_0$. In this subsection we want to calculate the value of A_0.

Before we start we note that in the case of constant activity A_0 and constant external input I_0, the total postsynaptic potential is also constant

$$h(t) = h_0 = J_0\, A_0 + J^{\text{ext}} I_0\,, \tag{10.48}$$

where we have used the normalization $\int \epsilon(s)ds = 1 = \int \tilde{\epsilon}(s)ds$.

Let us focus on the noise-free situation first. Given a constant input potential h_0, the neurons in the population fire with a period T_0 given by

$$\eta(T_0) = \vartheta - h_0\,. \tag{10.49}$$

Intuitively we expect that, if all neurons fire incoherently and with the same period T_0, then the population activity should be

$$A_0 = \frac{1}{T_0}\,. \tag{10.50}$$

(10.50) relies on the general ideal that, in a situation where everything is constant, averaging over time (for a single neuron) should be the same as

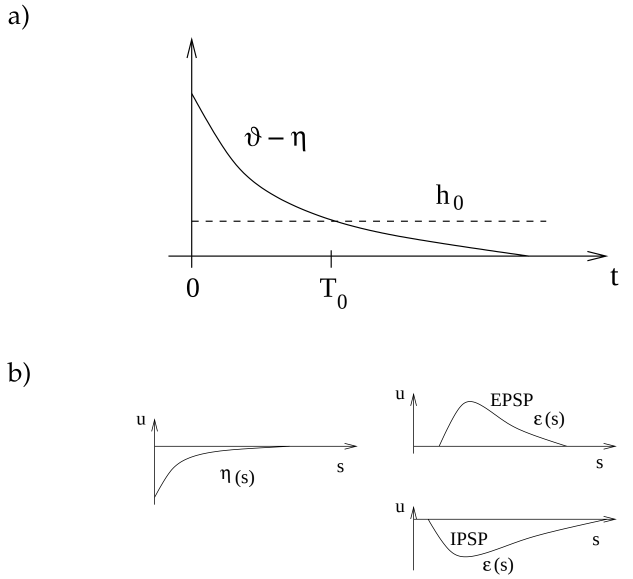

Figure 10.14. a) Determination of the interspike interval T_0 in case of incoherent firing. b) A plot of $1/T_0$ as a function of h_0 gives the gain function of the neuron (schematically).

averaging over a population of identical neurons. We will show in the following that, with the proper normalization defined in (10.25) our intuition and hence (10.50) are correct.

Moreover, the same consideration also holds in the noisy case. The population activity A_0 in an incoherent state must equal the mean firing rate ν,

$$A_0 = \nu = \frac{1}{\langle T \rangle} \tag{10.51}$$

where $\langle T \rangle$ is the mean interval length.

In order to show that (10.50) and (10.51) are correct, we start from the normalization (10.25). For constant input potential h_0, the survivor function $S_h(t \,|\, \hat{t})$ and the interval distribution $P_h(t \,|\, \hat{t})$ can not depend explicitly upon the absolute time, but only on the time difference $t - \hat{t}$. We set

$$\begin{aligned} S_0(s) &= S_{h_0}(\hat{t} + s \,|\, \hat{t}) \\ P_0(s) &= P_{h_0}(\hat{t} + s \,|\, \hat{t}) \end{aligned} \tag{10.52}$$

and from the definition of $S_h(t \,|\, \hat{t})$ in (10.23) we find

$$\frac{d}{ds} S_0(s) = -P_0(s)\,. \tag{10.53}$$

The normalization (10.25) reduces to

$$1 = A_0 \int_0^\infty S_0(s)\, ds\,. \tag{10.54}$$

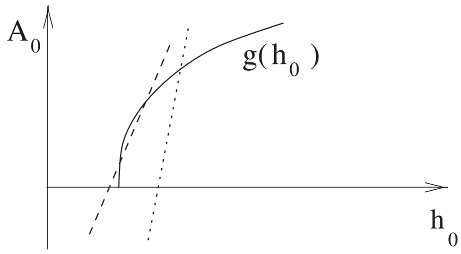

Figure 10.15. The intersection of the gain function $g(h_0)$ with the straight line $A_0 = [h_0 - J^{\text{ext}} I_0]/J_0$ gives the values of the activity A_0. Note that several solutions may coexist (dashed line).

Integrating (10.54) by parts yields

$$\begin{aligned} \frac{1}{A_0} &= \int_0^\infty 1\, S_0(s)\, ds \\ &= \int_0^\infty s\, P_0(s)\, ds \end{aligned} \tag{10.55}$$

since $s\, S_0(s)$ vanishes for $s = 0$ and $s \to \infty$. The term on the right-hand side of (10.55) is the first moment of the interval distribution, hence the *mean interval*

$$\langle T \rangle = \int_0^\infty s\, P_0(s)\, ds\,. \tag{10.56}$$

Thus, as promised above, for a given input potential h_0 the population activity is $A_0 = 1/\langle T \rangle$.

We recall that $P_0(s) = P_{h_0}(\hat{t} + s \,|\, \hat{t})$ is the interval distribution for constant input potential h_0. For our specific noise model, $P_0(s)$ is a Gaussian centered at the noise-free interval T_0

$$P_0(s) = \mathcal{G}_\sigma(s - T_0) \tag{10.57}$$

where σ is the width of the distribution. Thus, for this noise model,

$$A_0 = \frac{1}{\langle T \rangle} = \frac{1}{T_0} \tag{10.58}$$

as in the noise-free case. Equation (10.58) shows one of the advantages of the noise in the reset. For other noise models, the mean interval, and hence A_0, change with the level of noise. The expression (10.58) will prove rather useful for analysis of stability as a function of the noise-level.

We remark that the mean interval $\langle T \rangle$ depends on the input potential h_0. The relation is most easily understood in the noiseless case; cf. (10.49) and Figure 10.14. For each value of h_0 we have a solution T_0. If we plot the rate $1/T_0$ as a function of h_0, we get the gain function $g(h_0)$ of the neuron. Similarly, for the noisy case, we have

$$\nu = \frac{1}{\langle T \rangle} = g(h_0) \tag{10.59}$$

and with (10.51)

$$A_0 = g(h_0)\,. \tag{10.60}$$

As shown in (10.48), h_0 depends itself upon A_0. Thus, (10.60) is an implicit equation for A_0. A solution may be constructed graphically. It is convenient to transform (10.48) to

$$A_0 = \frac{1}{J_0}\,(h_0 - J^{\text{ext}} I_0)\,. \tag{10.61}$$

In Figure 10.15 we have plotted (10.60) and (10.61) as a function of h_0. The intersection points between the gain function (10.60) and the straight line defined by (10.61) gives potential solutions for A_0. This is just the same construction as for the Curie-Weiss theory of ferromagnetism which can be found in any physics textbook. More generally, the structure of the equations corresponds to a mean-field solution of a system with feedback.

As shown in Figure 10.15, several solutions may coexist, but it may also occur that *all* solutions are unstable. In the latter case, the network must leave the state of asynchronous firing and may evolve towards an oscillatory state. The stability analysis of the asynchronous state is the topic of the next subsection.

10.7.2 Stability of Asynchronous Firing

In this subsection we will analyze the stability of incoherent firing or 'splay state' [Chow, 1998]. The basic ideas is sketched in Figure 10.16. During asynchronous firing, the neuronal firing times are spread out over the full period T_0 which can be calculated from $h_0 = \vartheta - \eta(T_0)$. The characteristics of this state are clearly seen, if we order the neurons according their firing times. Due to the nice pattern, such a state has also been called a 'rotating wave' or a 'merry-go-round' state.

Let us now assume that the activity is subject to a small perturbation

$$A(t) = A_0 + A_1\, e^{i\omega t} \tag{10.62}$$

with $A_1 \ll A_0$. We have adopted a complex notation; the physical solution is, as usually, found by taking the real part. The perturbation in the activity induces a perturbation in the postsynaptic potential

$$\begin{aligned} h(t) &= J_0\, A_0 \int_0^\infty \epsilon(s) ds + J_0\, A_1 \left[\int_0^\infty \epsilon(s) e^{-i\omega s}\, ds\right] e^{i\omega t} \\ &= h_0 \qquad\qquad + \qquad h_1\, e^{-i\alpha(\omega)}\, e^{i\omega t} \end{aligned} \tag{10.63}$$

with

$$\begin{aligned} h_0 &= J_0 \hat{\epsilon}(0)\, A_0 \\ h_1\, e^{-i\alpha(\omega)} &= J_0 \hat{\epsilon}(\omega)\, A_1 \end{aligned} \tag{10.64}$$

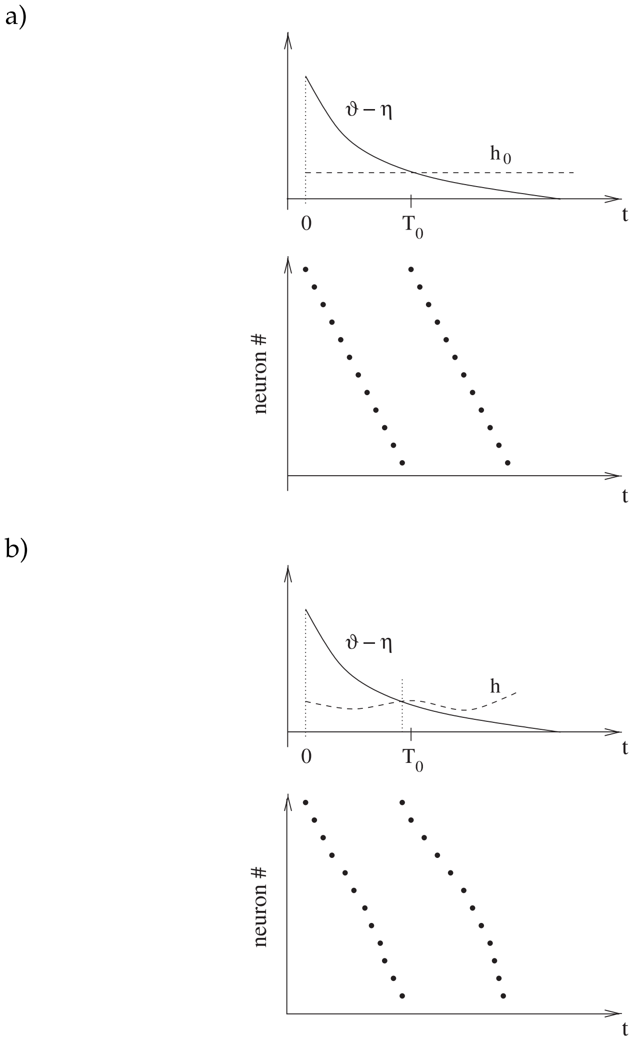

Figure 10.16. a) In an asynchronous state neuronal firing times are spread out maximally over the period T. The neurons have been ordered so that it is easy to see that they fire one after the other. b) In case of a small perturbation, neuronal firing times are no longer maximally spread out, but cluster slightly. This induces a perturbation in the field $h = h_0 + h_1 \cos\omega t$. As a result the neuronal firing times are shifted even more (vertical dashed line). This may lead to a build-up of a periodic perturbation.

where

$$\hat{\epsilon}(\omega) = |\hat{\epsilon}(\omega)|\, e^{-i\alpha(\omega)} = \int_0^{\infty} \epsilon(s)\, e^{-i\omega\, s}\, ds \tag{10.65}$$

is the Fourier transform of ϵ. (The lower bound of the integral can be extended to $-\infty$, since $\epsilon(s)$ vanishes for $s \leq 0$.)

The argument runs now as follows; cf. Figure 10.16. The periodic change in the potential causes some of the neurons to fire earlier (when the change in h is positive) others to fire later (whenever the change is negative). This

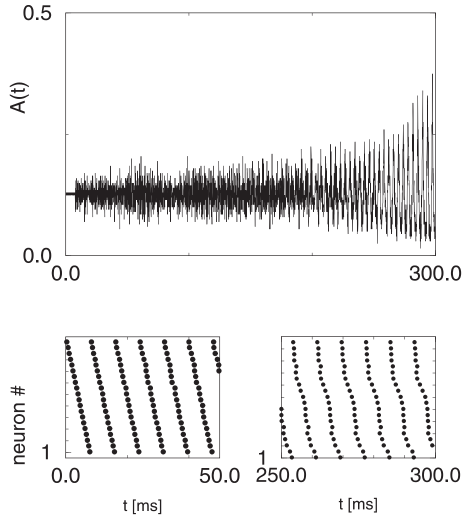

Figure 10.17. Simulation result. During the first 50 ms of the simulations, neuronal firing times are equally spread out (lower left). 250 ms later, there is a clear tendency that the firings cluster together which also shows up in an oscillation of the population activity. Parameters: excitatory coupling $J = 1$, delay $\Delta^{\text{ax}} = 3\,\text{ms}$, noise $\sigma = 0.05\,\text{ms}$.

may disturb the activity $A(t)$ even further and drive it away from the asynchronous state with constant A_0; cf. Figure 10.17. Whether this happens depends on the frequency ω of the perturbation and the phase shift α between the activity $A(t)$ and the potential $h(t)$. The exact conditions are derived in the following paragraphs. We apologize for the fact that the derivation is rather lengthy. Those readers who are not interested in the details of a mathematical argument may jump immediately to the paragraph labeled *results* further down below.

Mathematical steps We start from the general dynamic equation (10.17) for the population activity. On both sides of the equation, we put in our periodic Ansatz (10.62). Note that the interval distribution $P_h(t\,|\,\hat{t})$ depends on the potential h which changes due to the perturbation. We carefully expand to first order in h_1 or A_1 and find

$$\begin{aligned} A_0 + A_1\, e^{i\omega t} &= \int_{-\infty}^{t} \left[P_{h_0}(t\,|\,\hat{t}) + \frac{dP_h}{dh_1}(t\,|\,\hat{t})|_{h_1=0}\, h_1 \right] \left(A_0 + A_1\, e^{i\omega \hat{t}} \right) d\hat{t} \\ &= A_0 \int_{-\infty}^{t} P_0(t-\hat{t})\, d\hat{t} + A_1 \int_{-\infty}^{t} P_0(t-\hat{t})\, e^{i\omega\hat{t}}\, d\hat{t} \\ &\quad + h_1\, A_0 \int_{-\infty}^{t} \frac{dP_h}{dh_1}(t\,|\,\hat{t})|_{h_1=0}\, d\hat{t} \, + \mathcal{O}(h_1\, A_1)\,. \end{aligned} \tag{10.66}$$

After the second equality sign we have used (10.52) and omitted the second order term $\propto\, h_1 A_1$. As it should be, the zero-order terms cancel since $\int_{-\infty}^{t} P_0(t-\hat{t})d\hat{t} = \int_0^\infty P_0(s)ds = 1$. The second integral on the right-hand-side of (10.66) has a simple interpretation since it is the Fourier transform of the interval distribution

$$\begin{aligned}\int_{-\infty}^{t} P_0(t-\hat{t})\, e^{i\omega\hat{t}} d\hat{t} &= e^{i\omega t} \int_0^\infty P_0(s)\, e^{-i\omega s}\, ds \\ &= e^{i\omega t}\, \hat{P}(\omega)\,. \end{aligned} \tag{10.67}$$

This leaves us with

$$A_1\, e^{i\omega t} \left[1 - \hat{P}(\omega)\right] = A_0\, h_1 \int_{-\infty}^{t} \frac{dP_h}{dh_1}(t\,|\,\hat{t})|_{h_1=0}\, d\hat{t}\,. \tag{10.68}$$

Equation (10.68) is our first general result.

To treat the integral on the right-hand side of (10.68), we make the assumption of low noise. To understand the basic idea, let us consider the limit of no noise, first. A neuron which has fired at $\hat{t}$, fires again at $\hat{t} + T(\hat{t})$ given by the threshold condition

$$h[\hat{t} + T(\hat{t})] = \vartheta - \eta[T(\hat{t})]\,. \tag{10.69}$$

For a constant potential h_0, (10.69) yields the interval T_0. A change in the potential by $\delta h = h_1 e^{i\alpha}\, e^{i\omega t}$ shifts the firing time and hence the interval length. To first order in δh, the new interval is

$$\begin{aligned} T(\hat{t}) &= T_0 - \frac{\delta h(\hat{t} + T_0)}{\eta'(T_0)} \\ &= T_0 - \frac{h_1}{\eta'(T_0)}\, e^{i\alpha}\, e^{i\omega(\hat{t}+T_0)}\,. \end{aligned} \tag{10.70}$$

Note that for $\delta h > 0$ the interval gets shorter and for $\delta h > 0$ it gets longer, as expected from the sketch in Figure 10.16b.

In the case of a small amount of noise, the interval is not precisely determined, but has some distribution around the value $T(\hat{t})$ calculated in (10.70). We *assume* that, for a small amount of noise, the main effect of the perturbation is to shift the center of the interval distribution from the reference value T_0 to the perturbed value $T(\hat{t})$ calculated in (10.70). The approximation to the exact solution is expected to be good, if the width of the distribution is small compared to the period of the perturbation ($\omega\sigma \ll 1$). Thus we write

$$P_h(t\,|\,\hat{t}) = P_0\left(t - \hat{t} + \frac{h_1}{\eta'} e^{-i\alpha}\, e^{i\omega(\hat{t}+T_0)}\right)\,. \tag{10.71}$$

With (10.71) the integral on the right-hand side of (10.68) can be solved using integration by parts. To do so, we note that because of (10.71)

$$\begin{aligned} \frac{d}{dh_1} P_h(t\,|\,\hat{t})|_{h_1=0} &= \frac{d}{dh_1} P_0\left(t - \hat{t} + \frac{h_1}{\eta'} e^{-i\alpha}\, e^{i\omega(\hat{t}+T_0)}\right) |_{h_1=0} \\ &= -\frac{d}{d\hat{t}} P_0(t-\hat{t})\, \frac{1}{\eta'} e^{-i\alpha}\, e^{i\omega(\hat{t}+T_0)}\,. \end{aligned} \tag{10.72}$$

With view to (10.68), we integrate (10.72)

$$\int_{-\infty}^{t} \frac{d}{dh_1} P_h(t\,|\,\hat{t})|_{h_1=0}\, d\hat{t} = \frac{i\omega}{\eta'} e^{-i\alpha}\, e^{i\omega T_0}\, \hat{P}(\omega)\, e^{i\omega t}\,. \tag{10.73}$$

After all these transformations, we may now use (10.73) on the right-hand side of (10.68) and arrive at our final result

$$1 - \hat{P}(\omega) = \frac{i\omega}{\eta'} J_0 \, A_0 \, e^{i\omega T_0} \hat{\epsilon}(\omega) \, \hat{P}(\omega) \tag{10.74}$$

where we have used $h_1 e^{-i\alpha} = J_0 \, A_1 \, \hat{\epsilon}(\omega)$ and cancelled the common factor $A_1 \, e^{i\omega t}$ on both sides of the equation.

Equation (10.74) is an approximative result which was derived on the assumption that the perturbation only shifts the center of the distribution, but does not change its form. In [Gerstner, 1998] a different approach is taken which does not rely on this assumption. The resulting equation is somewhat different from (10.74). The regions of stability and the qualitative structure of the solutions are, however, unchanged and we will therefore use (10.74) for the following discussion.

Application The result (10.74) is quite general. We now want to apply it to our specific model.

With Gaussian noise in the reset, the interval distribution is a Gaussian centered at T_0,

$$P_0(s) = \mathcal{G}_\sigma(s - T_0) = \frac{1}{\sqrt{2\pi}} \frac{1}{\sigma} \exp\left[-\frac{(s - T_0)^2}{2\sigma^2}\right] . \tag{10.75}$$

We need the Fourier transform

$$\hat{P}(\omega) = \exp\left[-\frac{1}{2}\sigma^2 \, \omega^2\right] \, e^{-i\omega T_0} \, . \tag{10.76}$$

The maximum of $|\hat{P}|$ is at $\omega = 0$ and has the value $|\hat{P}(0)| = 1$ independent of σ. In the limit of no noise ($\sigma \to 0$) the interval distribution is $P_0(s) = \delta(s - T_0)$ and $|\hat{P}(\omega)| \equiv 1$.

We also need to specify the response kernel ϵ. The Fourier transform of (10.6) is

$$\hat{\epsilon}(\omega) = |\hat{\epsilon}(\omega)| \, e^{-i\alpha(\omega)} \tag{10.77}$$

with amplitude and phase

$$\begin{aligned} |\hat{\epsilon}(\omega)| &= \frac{1}{(1 + \omega^2 \, \tau^2)} \\ \alpha(\omega) &= \omega \, \Delta^{\mathrm{ax}} + 2 \arctan(\omega \, \tau) \, . \end{aligned} \tag{10.78}$$

We note that a change in the delay Δ^{ax} only affects the *phase* of the Fourier transform and not the amplitude. This is a convenient property which we will exploit later.

Furthermore, we need the derivative of the response kernel η. We take the kernel (10.8) and therefore

$$\eta'(T_0) = \frac{\eta_0}{T_0} \, \exp\left(-\frac{T}{\tau}\right) \, . \tag{10.79}$$

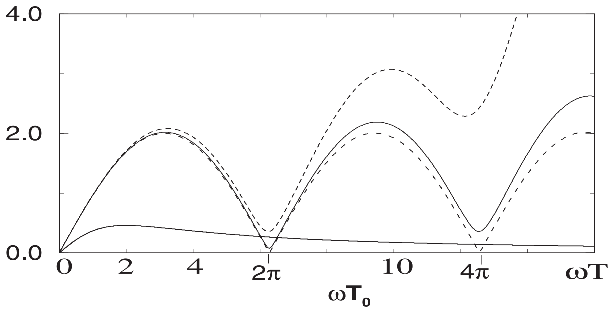

Figure 10.18. Graphical solution of the amplitude condition for bifurcation of an oscillatory solution. The crossing points lie at frequencies $\omega \approx \omega_n = n\,2\pi/T_0$. For the plot we have set $T_0 = 2\tau$, $J_0 = \eta_0 = 1$ which yields a factor of $C = 0.92$. Three values of noise are shown. For $\sigma = 1.0$ ms (long dashed curve, top), no crossing point except the one at $\omega = 0$ exists. For $\sigma = 0.5$ ms (thin solid line), two solutions of the amplitude condition with $\omega\tau = 2\pi \pm \delta$ with $\delta \ll 1$ exist. For $\sigma = 0.1$ ms (dotted line), crossing points at $\omega T_0 \approx 2\pi$ and 4π are shown. The thick solid line is $C\,\hat{f}(x)$ with $\hat{f}(x) = x/(1+x^2)$ and $C = 0.92$; adapted from [Gerstner and Van Hemmen, 1995].

Let us now collect the various terms from (10.8), (10.76), (10.78), and (10.79) and put them into (10.74). The result is

$$\exp\left[-\frac{1}{2}\sigma^2\,\omega^2\right] - e^{-i\omega T_0} = C\,e^{-i(\alpha-\frac{\pi}{2})}\,\frac{\omega\tau}{1+\omega^2\,\tau^2} \tag{10.80}$$

with a factor

$$C = \frac{J_0}{\eta_0\,\tau}\exp\left(\frac{T_0}{\tau}\right). \tag{10.81}$$

Are there frequencies ω so that (10.80) has a solution? To check this, we take the absolute value on both sides of (10.80)

$$\left[1+\exp\left(\sigma^2\,\omega^2\right) - 2\cos(\omega\,T_0)\,\exp\left(\frac{\sigma^2\,\omega^2}{2}\right)\right]^{1/2} = C\,\frac{\omega\tau}{1+\omega^2\,\tau^2} \tag{10.82}$$

and plot both the left-hand side and the right-hand side as a function of ω; cf. Figure 10.18. For $\sigma \to 0$ the left-hand side is $2|\sin(\omega T_0/2)|$ and solutions are possible only for frequencies $\omega \approx \omega_n = n\,2\pi/T_0$ with integer n. A solution with ω_1 implies that the period of the population activity is identical to the period of individual neurons. The other solutions correspond to higher harmonics. We see from Figure 10.18 that higher harmonic solutions disappear at some finite noise level. At high noise level, even the solution $\omega \approx \omega_1$ disappears.

Equation (10.82) only gives an *amplitude* condition for solution of (10.80). In order to derive the phase equations, we have to work a little bit harder. Since we now know that solutions are possible only for $\omega \approx \omega_n$, we set

$$\omega = \omega_n + \nu_n\,. \tag{10.83}$$

Furthermore, for $n \geq 1$ and $T = 2\tau$, we have $\omega_n\tau = n\,\pi > 3$ and we can approximate the $\arctan$ in (10.78) by $\arctan(x) \approx (\pi/2) - (1/x)$. The phase factor in (10.80) is therefore

$$\alpha - \frac{\pi}{2} = \omega\, \Delta^{\rm ax} - \frac{2}{\omega\,\tau} + \frac{\pi}{2}\,. \tag{10.84}$$

The aim is now to write down conditions for the real and the imaginary part of (10.80). In order to simplify the notation, we set

$$\begin{aligned} \hat{f}(\omega) &= \frac{\omega\,\tau}{1+\omega^2\,\tau^2} \\ \hat{g}(\omega) &= \exp\left(\frac{1}{2}\sigma^2\,\omega^2\right) \end{aligned} \tag{10.85}$$

Furthermore we note that, because of (10.83), the phases simplify $i\omega T_0 = i\nu_n T_0$. Grouping the real and the imaginary part of (10.80) in two equations yields

$$\begin{aligned} \hat{g}(\omega) - \cos(\nu_n\, T_0) &= C\,\hat{f}(\omega)\,\sin\psi \\ \sin(\nu_n\, T_0) &= -C\,\hat{f}(\omega)\,\cos\psi \end{aligned} \tag{10.86}$$

with $\psi = (2/\omega\tau) - \omega\Delta^{\rm ax}$. We have solved (10.86) numerically for different values of the delay $\delta^{\rm ax}$ and different levels of the noise σ. The results are shown in Figure 10.19 and discussed in the next paragraph.

Results We have studied a population of neurons with ϵ given by (10.6) and η by (10.8). Neurons interact with strength $J_0 = 1$ and The value of the threshold ϑ was adjusted so that $T = 2\tau$. In our simulations we have taken $\tau = 4$ ms and a total number of $N = 1000$ neurons.

The results of our analytical stability analysis are shown in the phase diagram in the center of Figure 10.19. The y-axis is the level of noise, the x-axis the value of the axonal transmission delay devided by the interspike interval T_0. Let us study a network with interaction delay $\Delta^{\rm ax} = 2$ ms. This corresonds to a x-value of $\Delta^{\rm ax}/T_0 = 0.25$ in Fig, 10.19. The phase diagram predicts that, at a noise level of $\sigma = 0.5$ ms, the network is in a state of asynchronous firing. The activity during a simulation run is shown in the inset in the upper right-hand corner. It confirms that the activity fluctuates around a constant value of $A_0 = 1/T_0 = 0.125$ kHz.

We imagine now that we reduce the noise level of the network. At some point we cross the short-dashed line. The line is the boundary at which the constant activity state becomes unstable with respect to an oscillation with $\omega \approx 3\,(2\pi/T_0)$. A simulation result for a network at a noise level of $\sigma = 0.1$, but otherwise the same parameters as before confirms that the population activity exhibits an oscillation with period $T^{osc} \approx T_0/3 \approx 2.6$ ms.

Let us return to our original parameters of $\sigma = 0.5$ ms and $\Delta^{\rm ax} = 2$ ms. We now keep the noise level fixed and reduce the axonal transmission delay. In this case we move horizontally across the phase diagram in Figure 10.19. At some point, we cross the solid line which marks the transition to an instability with frequency $\omega_1 = 2\pi/T_0$. Again this is confirmed by the simulation results shown in the inset in the upper left corner. If we now decrease the noise level, the oscillation becomes more pronounced (bottom right).

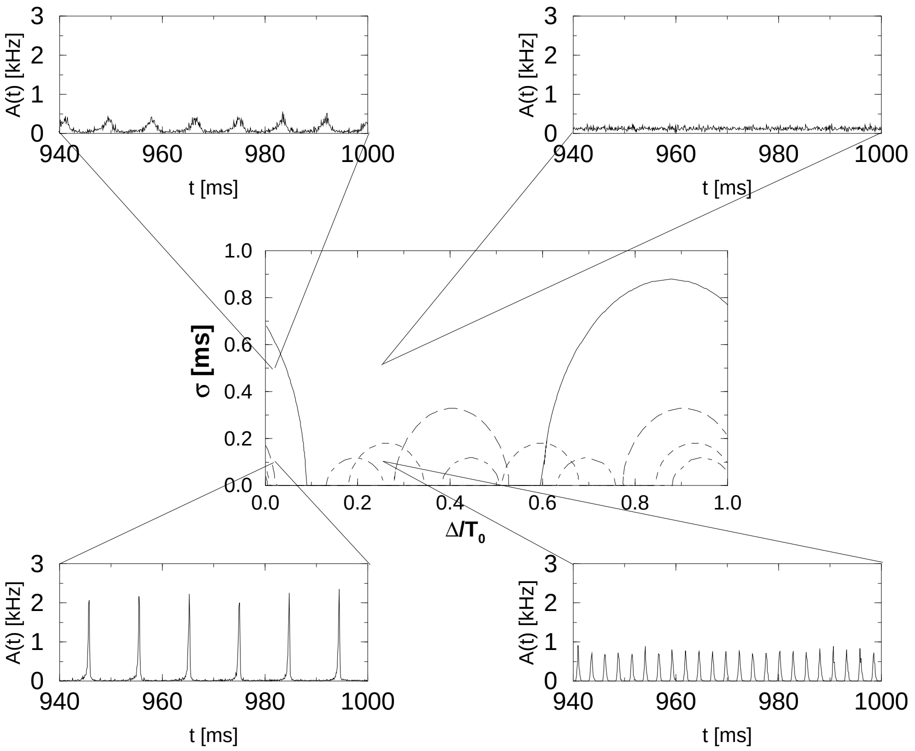

Figure 10.19. Stability diagram (center) as a function of noise σ (y-axis) and delay $\Delta^{\rm ax}$ (x-axis). The diagram shows the borders of the stability region with respect to $\omega_1, \dots, \omega_4$. For high values of the noise, the asynchronous firing state is always stable. If the noise is reduced, the asynchronous state becomes unstable with respect to an oscillation either with frequency ω_1 (solid border lines), or ω_2 (long-dashed border lines), or ω_3 (short-dashed border lines), or ω_4 (long-short dashed border lines). Four insets shows typical patterns of the activity as a function of time taken from a simulation with 1000 neurons. Parameters $\sigma = 0.5$ ms and $\Delta^{\rm ax} = 0.2$ ms (top left); $\sigma = 0.5$ ms and $\Delta^{\rm ax} = 2.0$ ms (top right); $\sigma = 0.1$ ms and $\Delta^{\rm ax} = 0.2$ ms (bottom left); $\sigma = 0.1$ ms and $\Delta^{\rm ax} = 2.0$ ms (bottom right); Since the pattern repeats along the x-axis with period T_0, we have plotted a normalized delay $\Delta^{\rm ax}/T_0$. Adapted from [Gerstner, 1998].

For practically all values of the delay, the incoherent network state is unstable in the limit of no noise ($\sigma \to 0$). This is exemplified in Figure 10.20 where we have explored different values of the delay for a constant noise level $\sigma = 0.04$ ms. For a very short delay, the network oscillates with frequency of about ω_1, increasing the delay it passes through oscillations with ω_6, ω_5, ω_4, ω_3, and ω_2.

We emphasize that the specific location of the stability borders depends on the form of the postsynaptic response function ϵ. The qualitative features of the phase diagram in Figure 10.19 are generic and hold for all kinds of response kernels.

Finally, what happens if the excitatory interaction is replaced by inhibitory coupling? Not much. For each harmonic, the region along the delay axis where the incoherent state is *unstable* for excitatory coupling (cf. Fig-

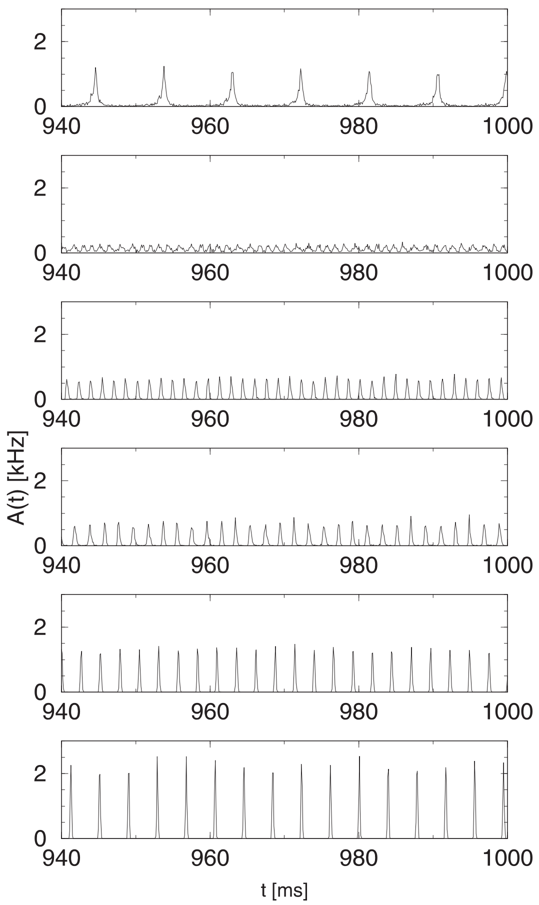

Figure 10.20. Activity for different values of the delay at a low noise level ($\sigma = 0.04$ ms). From top to botton: $\Delta^{\rm ax}$ = 0.4ms; 1.0 ms; 1.2 ms; 1.4 ms; 2.0 ms; 3.0 ms. Taken from [Gerstner, 1998].

ure 10.19) becomes *stable* for inhibition and vice versa. In other words, we simply have to shift the instability tongues for each frequency ω_n horizontally by an amount $\Delta/T_0 = 1/(2n)$. Otherwise the pattern remains the same.

10.8 Conclusions

We have seen that the population activity in a homogeneous population of neurons can be described by an integral equation. A description by differential equations of the form (10.2) is, in general, not possible. A systematic reduction of the integral equation to a single differential equation of the form (10.2) always supposes that the activity changes only *slowly* compared to the typical interval length [Wilson and Cowan, 1972, Gerstner, 1995, Pinto et al., 1996]. The existence of perfectly synchronized oscillations and the fast initital transients discussed in this contribution, clearly show that an assumption of slow changes is, in general, not justified. It seems therefore preferable to work directly on the level of the integral equation. A useful approximation might be to describe the activity of a single population by a set of several coupled differential equations [Gerstner, 1993; Eggert and van Hemmen, 1997].

The population equation (10.17) is valid for neurons with short memory, i.e., only the most recent spike matters. More generally, the condition of short memory leads to the class of renewal models [Perkel et al., 1967, Stein, 1967, Cox, 1962] and this is where the integral equation applies; cf. [Gerstner, 1995]. A generalization to neuron models with longer memory, in particular adaptation, does not seem straightforward.

One of the solution of the integral equation is that of neurons firing in perfect synchrony. The synchronous solution is stable, if the input potential h is increasing in the moment of firing. This is the essence of the locking theorem [Gerstner et al., 1996]. The locking theorem is a special case of a more general property of the integral equation: firing times are compressed and, hence, the activity increases, whenever firing occurs while the input potential is rising ($h' > 0$).

Another solution of the integral equation is the state of incoherent firing. If the network is firing incoherently, then the population acitivity responds immediately to an abrupt change in the input [Tsodyks and Sejnowski, 1995, van Vreeswijk and Sompolinsky, 1996]. There is no integration delay. In the case of incoherent firing, there are always *some* neurons close to threshold – and this is why the system as a whole can respond immediately. This property suggests that a population of neurons may transmit information fast and reliably. Fast information processing seems to be a necessary requirement for biological nervous systems, if the reaction time experiments are to be accounted for [Thorpe et al., 1996].

It follows that the state of incoherent firing may be particularly interesting for information transmission. Incoherent firing can be stabilized by a suitable choice of time constants, transmission delay, and noise. [Abbott and van Vreeswijk, 1993; Gerstner and van Hemmen, 1993, 1994; Gerstner, 1995]. For low noise, incoherent states are *unstable* for nearly all choices of parameters. Instabilities lead towards oscillations, either with a period comparable to the typical interval of the neuronal spike trains, or much faster (higher harmonics) [Golomb et al., 1992, Gerstner and van Hemmen, 1993, Ernst et al., 1994, Golomb and Rinzel, 1994]. The harmonics have also been called cluster states since neurons spontaneously split into groups of neurons which fire approximately together. The higher harmonics can be easily suppressed by noise.

Finally, we would like to emphasize that there are no completely homogeneous populations in biology. The population equations discussed in this chapter may nevertheless be a useful starting point for a theory of heterogeneous populations [Senn et al., 1996, Chow, 1998]. We expect that most of the results discussed in the present chapter also hold for nonhomogeneous networks.

References

[Abbott and van Vreeswijk, 1993] Abbott, L. F. and van Vreeswijk, C. (1993). Asynchronous states in a network of pulse-coupled oscillators. *Phys. Rev. E*, 48:1483–1490.

[Amari, 1974] Amari, S. (1974). A method of statistical neurodynamics. *Kybernetik*, 14:201–215.

[Bauer and Pawelzik, 1993] Bauer, H. U. and Pawelzik, K. (1993). Alternating oscillatory and stochastic dynamics in a model for a neuronal assembly. *Physica D*, 69:380–393.

[Chow, 1998] Chow, C. C. (1998) Phase-locking in weakly heterogeneous neuronal networks. *preprint*.

[Cohen and Grossberg, 1983] Cohen, M. A. and Grossberg, S. (1983). Absolute stability of global pattern formation and parallel memory storage by competitive neural networks. *IEEE trans. on systems, man, and cybernetics*, 13:815–823.

[Cox, 1962] Cox, D. R. (1962). *Renewal Theory*. Mathuen, London.

[Eggert, 1997] Eggert, J. (1997). Derivation of pool dynamics from microscopic neuronal models. *Artificial Neural Networks* - ICANN'97, W. Gerstner, A. Germond, M. Hasler, and J.-D. Nicoud, eds., Springer-Verlag, 109–114.

[Ernst et al., 1994] Ernst, U., Pawelzik, K., and Geisel, T. (1994). Multiple phase clustering of globally coupled neurons with delay. *Proc. of the ICANN'94*, M. Marinaro and P. G. Morasso, eds., Springer-Verlag, Berlin Heidelberg New York, 1063–1065.

[Gerstner, 1993] Gerstner, W. (1993). *Kodierung und Signalübertragung in Neuronalen Systemen: Assoziative Netzwerke mit stochastisch feuernden Neuronen*, volume 15 of *Reihe Physik*. Harri–Deutsch Verlag, Frankfurt/Main, 1993. Dissertation Nov. 1992, TU München.

[Gerstner, 1995] Gerstner, W. (1995). Time structure of the activity in neural network models. *Phys. Rev. E*, 51(1):738–758.

[Gerstner, 1998] Gerstner, W. (1998) Population dynamics for spiking neurons: fast transients, asynchronous states and locking. *preprint*, 1997.

[Gerstner et al., 1993] Gerstner, W., Ritz, R., and van Hemmen, J. L. (1993). A biologically motivated and analytically soluble model of collective oscillations in the cortex: I. theory of weak locking. *Biol. Cybern.*, 68:363–374.

[Gerstner and van Hemmen, 1992] Gerstner, W. and van Hemmen, J. L. (1992). Associative memory in a network of 'spiking' neurons. *Network*, 3:139–164.

[Gerstner and van Hemmen, 1993] Gerstner, W. and van Hemmen, J. L. (1993). Coherence and incoherence in a globally coupled ensemble of pulse emitting units. *Phys. Rev. Lett.*, 71(3):312–315.

[Gerstner and van Hemmen, 1994] Gerstner, W. and van Hemmen, J. L. (1994). Coding and information processing in neural networks. In *Models of neural networks II*, E. Domany, J. L. van Hemmen, and K. Schulten, eds., Springer-Verlag, New York, 1–93.

[Gerstner et al., 1996] Gerstner, W., van Hemmen, J. L., and Cowan, J. D. (1996). What matters in neuronal locking. *Neural Computation*, 8:1689–1712.

[Golomb et al., 1992] Golomb, D., Hansel, D., Shraiman, B., and Sompolinsky, H. (1992). Clustering in globally coupled phase oscillators. *Phys. Rev. A*, 45:3516–3530.

[Golomb and Rinzel, 1994] Golomb, D. and Rinzel, J. (1994). Clustering in globally coupled inhibitory neurons. *Physica D*, 72:259–282, 1994.

[Hansel et al., 1995] Hansel, D., Mato, G., and Meunier, C. (1995). Synchrony in excitatory neural networks. *Neural Computation*, 7:307–337.

[Hopfield, 1984] Hopfield, J. J. (1984). Neurons with graded response have computational properties like those of two–state neurons. *Proc. Natl. Acad. Sci. USA*, 81:3088–3092.

[Hopfield and Herz, 1995] Hopfield J. J. and Herz, A. V. M. (1995). Rapid local synchronization of action potentials: towards computation with coupled integrate-and-fire networks. *Proc. Natl. Acad. Sci. USA*, 92:6655.

[Mirollo and Strogatz, 1990] Mirollo, R. E. and Strogatz, S. H. (1990). Synchronization of pulse coupled biological oscillators. *SIAM J. Appl. Math.*, 50:1645–1662.

[Perkel et al., 1967] Perkel, D. H., Gerstein, G. L., and Moore, G. P. (1967). Neuronal spike trains and stochastic point processes. (i) the single spike train. *Biophys. J.*, 7:391–418.

[Pinto et al., 1996] Pinto, D. J., Brumberg, J. C., Simons, D. J., and Ermentrout, G. B. (1996). A quantitative population model of whiskers barrels: re-examining the Wilson-Cowan equations. *J. Comput. Neurosci.*, 3:247–264.

[Senn et al., 1996] Senn, W., Wyler, K., Streit, J., Larkum, M., Lüscher, H.-R., Mey H., Müller, L., Steinhauser, D., Vogt, K., and Wannier, T. (1996). Dynamics of random neural network with synaptic depression. *Neural Networks*, 9:575–588.

[Somers and Kopell, 1993] Somers, D. and Kopell, N. (1993). Rapid synchronization through fast threshold modulation. *Biol. Cybern.*, 68:393–407.

[Stein, 1967] Stein, R. B. (1967). Some models of neuronal variability. *Biophys. J.*, 7:37–68.

[Terman and Wang, 1995] Terman, D. and Wang, D. (1995). Global competition and local cooperation in a network of neural oscillators. *Physica D*, 81:148–176.

[Thorpe et al., 1996] Thorpe, S., Fize, D., and Marlot, C. (1996). Speed of processing in the human visual system. *Nature*, 381:520–522.

[Tsodyks and Sejnowski, 1995] Tsodyks, M. V. and Sejnowski, T. (1995). Rapid state switching in balanced cortical networks. *Network*, 6:111–124.

[van Vreeswijk and Sompolinsky, 1996] van Vreeswijk, C. and Sompolinsky, H. (1996). Chaos in neuronal networks with balanced excitatory and inhibitory activity. *Science*, 274:1724–1726.

[van Vreeswijk et al., 1994] van Vreeswijk, C., Abbott, L. F., and Ermentrout, G. B. (1994). When inhibition not excitation synchronizes neural firing. *Journal of Computational Neuroscience*, 1:313–321.

[Wilson and Cowan, 1972] Wilson, H. R. and Cowan, J. D. (1972). Excitatory and inhibitory interactions in localized populations of model neurons. *Biophysical J.*, 12:1–24.

[Wilson and Cowan, 1973] Wilson, H. R. and Cowan, J. D. (1973). A mathematical theory of the functional dynamics of cortical and thalamic nervous tissue. *Kybernetik*, 13:55–80.